Morphology and Crystallization Behavior of the PP/PET Nanocomposites

Carmen I. W. Calcagno,[1,2] Cleide M. Mariani,[1] Sérgio R. Teixeira,[3] Raquel S. Mauler[1]

[1]*Instituto de Quimica - PGCIMAT, Universidade Federal do Rio Grande do Sul, Av. Bento Gonçalves, 9500, Porto Alegre/RS 91501-970, Brazil*
[2]*CEFET/RS, Av. Copacabana, 100, 93216-120, Sapucaia do Sul, Brazil*
[3]*Instituto de Fisica - PGCIMAT, Universidade Federal do Rio Grande do Sul, Av. Bento Gonçalves, 9500, Porto Alegre/RS 91501-970, Brazil*

Received 10 May 2007; accepted 14 May 2008
DOI 10.1002/app.28977
Published online 26 September 2008 in Wiley InterScience (www.interscience.wiley.com).

ABSTRACT: Nanocomposites containing polypropylene (PP), PET, and montmorillonite were prepared in a twin-screw extruder. X-ray diffraction, transmission electron microscopy, scanning electron microscopy, atomic force microscopy, polarized optical microscopy, and differential scanning calorimetry were used to characterize the samples. Intercalated and exfoliated morphology were observed in the nanocomposites. The PET domains usually presented spherical shapes and they were the start point to PP crystallization. The average diameter and number of PET domains was evaluated. The influence of addition of PP-MA as compatibilizer on PP/PET was investigated. The interconnected morphology was observed in the nanocomposite containing PP-MA. The clay located predominantly in the interphase and in the PET phase. The crystallization process was monitored and the PET crystallization rate was slower in the nanocomposites. © 2008 Wiley Periodicals, Inc. J Appl Polym Sci 111: 29–36, 2009

Key words: nanocomposite; PP/PET blend; crystallization

INTRODUCTION

Polypropylene (PP), is one of the most important type of thermoplastics used in industrial processes. The growth of its importance is attributed to its attractive combination of low cost, low density, and high heat distortion temperature (HDT). However, there are always certain shortcomings in physical and chemical properties that can limit the universal use of any given polymer.

Polymer blending is a useful technique to generate materials with specific enhanced properties. The blending of polyolefins with engineering plastics is a route to improve the mechanical properties of polymeric materials. Another route that has been widely used is based on the development of nanocomposites.

Nanocomposites use low filler content (usually <6%) and show extraordinary advantages in the mechanical, thermal, optical, and physicochemical properties when compared to the pure polymer or the conventional composites (with micrometer particles sizes).[1,2] Silicates, like montmorillonite (MMT), have been used for nanocomposites preparation owing to their high aspect ratio (size/thickness) and unique intercalation/exfoliation characteristics. The improvement in nanocomposites properties is directly correlated with the exfoliation/dispersion of the nanoclay layers within the polymeric matrix. There are several techniques used for dispersing clay at a nanoscopic scale, as *in situ* intercalative polymerization; solvent swollen polymer (solution blending); or melt intercalation method, as described in recent reviews.[1–4]

The dispersion of the clay into polyolefins was found to be a key step in the preparation of nanocomposites. Because of the low polarity of PP, it is difficult to get the exfoliation and homogeneous dispersion of the silicate layer at the nanometer level in the polymer. Several tentative have been done to obtain polyolefin nanocomposites and most of them result in intercalated morphology.[5,6] Nevertheless, polymer/clay nanocomposites have experienced some success in several kinds of polar polymers and the blending of a polar and an apolar thermoplastic polymer appeared, therefore, to be promising.[7–15]

The PP/PET blend development has importance due its potential for some applications in engineering. The addition of PET in PP results in elastic modulus increase and improvement in the mechanical properties.[16] However, no study on nanocomposites containing these two polymers was found.

Most chemically different polymers are immiscible and their blending leads to materials with weak interfacial adhesion and poor mechanical performances. It is difficult to obtain good dispersion in polymer

Correspondence to: R. S. Mauler (mauler@iq.ufrgs.br).
Contract grant sponsor: The Conselho Nacional de Desenvolvimento Científico e Tecnológico-CNPq, Pronex/FAPERGS.

TABLE I
Thermal and Crystallization Behavior of PP/PET Blends

	Composition (wt %)				Basal distance (Å)	PET domains size (μm)	PET domains/mm^2	T_m (°C)[a]		T_c (°C)[a]		Crystallinity (%)	
	PP	PET	PP-MA	Clay				PP	PET	PP	PET	PP	PET
PP	100	–	–	–	–	–	–	163	–	122	–	36	–
PET		100	–	–	–	–	–	–	247	–	184	–	24
PP/PET	70	30	–	–	–	6.3 ± 3.2	9598	162	246	119	187	47	21
PP/PET/clay	70	28	–	2	44.1	4.0 ± 2.6	18,471	160	247	117	189	41	19
PP/PET/PP-MA	70	29	1	–	–	2.7 ± 1.5	27,974	162	247	118	188	45	23
PP/PET/PP-MA/clay	70	27	1	2	–	Interconnected morphology	Interconnected morphology	161	246	117	190	47	20

[a] Determined by DSC.

blends, particularly for combinations of nonpolar with polar polymers. The conversion of the immiscible blend to a useful polymeric product with desired properties requires some modifications of their interfaces. The compatibilization produces the desired blend morphology by controlling the interfacial properties, and thus the size of the dispersed droplets of the minor phase. The stabilization of the morphology prevents the coalescence during the subsequent processing steps, as well as, it ensures adhesion between the phases in the solid state, thus improving the mechanical properties.[15] Maleic anhydride modified polypropylene, PP-MA, is often used as compatibilizer or adhesion promoter in various heterogeneous polymer systems.[14,17–21]

In the present study, it was developed different blends of PP and PET by using the direct melt blending technique. Nanocomposites containing PP, PET, and MMT were prepared and the influence of the clay and compatibilizer addition into the PP/PET blend was investigated. The characterization of the samples was carried out using Wide Angle X-Ray Diffraction (WAXD), Transmission Electron Microscopy (TEM) Scanning Electron Microscopy (SEM), Polarized Optical Microscopy (POM), Atomic Force Microscopy (AFM), and Scanning Differential Calorimetry (DSC).

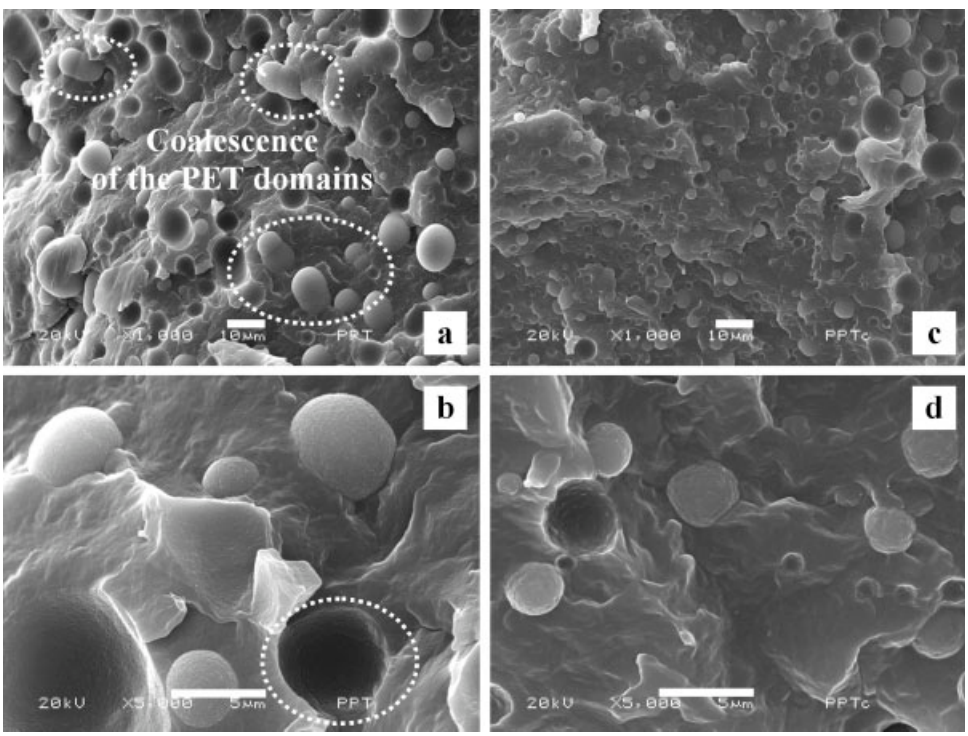

Figure 1 Morphology of PET domains in the PP/PET (a,b) and PP/PET//PP-MA (c,d).

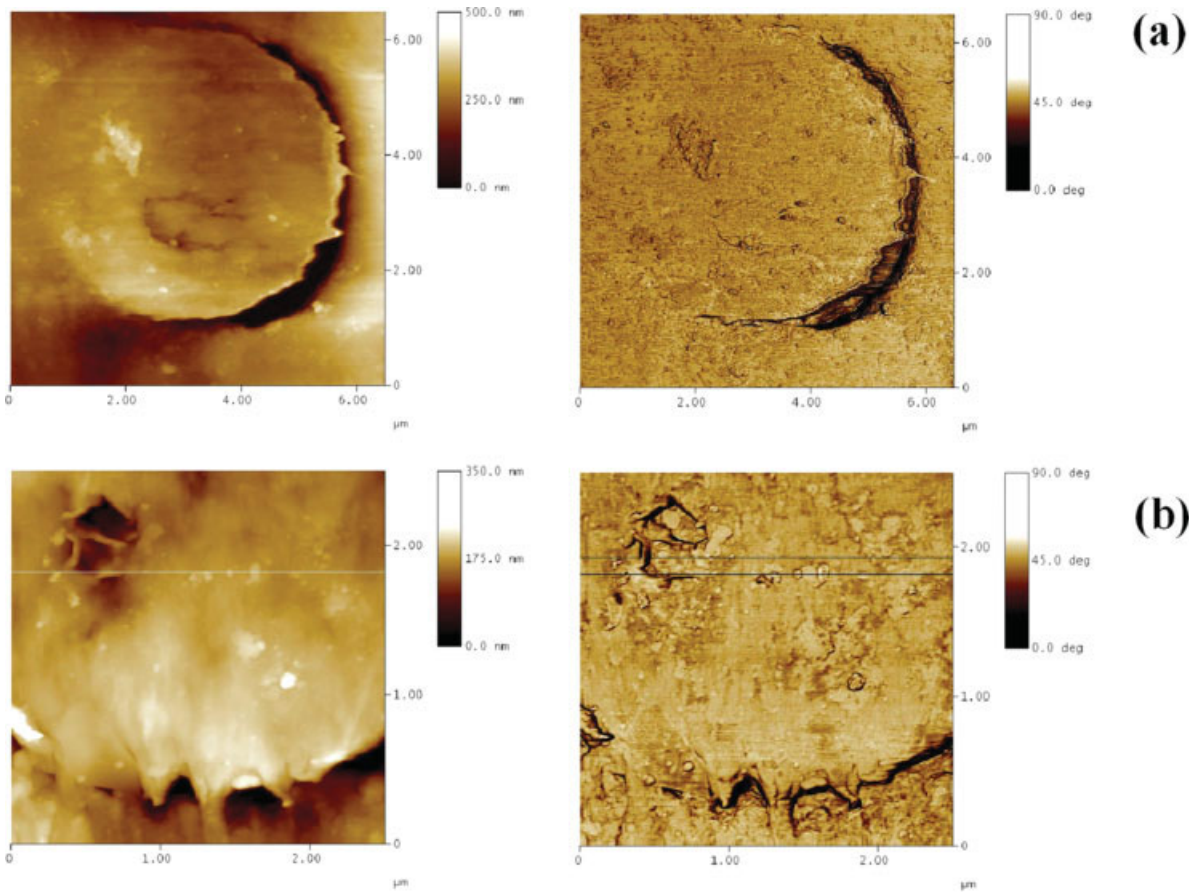

Figure 2 AFM of the (a) PP/PET and (b) PP/PET/PP-MA blends. Topographic AFM (left) and Phase AFM (right). [Color figure can be viewed in the online issue, which is available at www.interscience.wiley.com.]

EXPERIMENTAL

Materials

PP (MFI = 3,5-Braskem); PET (RHOPET *S*-80/Rhodia-Ster-Mossi and Ghisolfi Group); maleic anhydride grafted polypropylene, PP-MA (polybond® 3002-Crompton) and commercial MMT (Cloisite® 10A-Southern Clay Products) were used as received. PET and MMT were dried at 140°C, under vacuum, for ~ 4 h.

Melt processing

PP, PET, PP-MA, and MMT were processed in a twin screw extruder (Haake H-25, model Rheomex PTW 16/25, $L/D = 25$), using a temperature profile of 225–245°C in the die. The screw speed was 50 rpm. The compositions are showed in Table I. In all samples 0.2% of antioxidant (IB215-CIBA) was used to prevent degradation of the PP during the mixture process.

Characterization

Films and specimens were obtained by compression, heating the polymer up to 260°C, and maintaining this temperature for 5 min to obtain the complete melt of the pellets. After that, a pressure of 100 lbs was applied for 5 min. The sample was then cooled to room temperature at a cooling rate of around 20°C/min. Similar conditions were used to obtain thicker specimens using decompression/compression for the elimination of air bubbles.

WAXD experiments were performed in a Siemens D-500 diffractometer. The films were scanned in the Bragg-Brentano reflection mode using a CuK_α radiation ($\lambda = 1.5406$ Å) with a step size of 0.05°/min from $2\theta = 1$ to 10°. The space gallery was determined for the clay and nanocomposites using the Bragg's law.

TEM micrographs were obtained in a JEOL JEM-120 EXII TEM microscope operating at an accelerating voltage of 80 kV using ultrathin cuts from the compressed specimens. The cuts were placed on 300 mesh Cu grids.

SEM experiments were performed in a Jeol JSM 6060 to examine the shape and the size of the dispersed phase. The observed surfaces were obtained by criogenic fracture of the films after covered with gold. Four SEM photomicrographs (magnification 1000×) were analyzed for each sample to calculate the average diameter and number of PET domains

per area. The distribution curves of PET particles diameter in PP were evaluated.

POM observation was performed using a Olympus-BX41 microscope using 40× lens. POM experiments were carried out by heating the films to 250°C and holding them for 5 min at this temperature. The crystallization was monitored during the cooling process.

Thermal and crystallization behavior were determined using DSC Perkin–Elmer instruments. The temperature and energy readings were calibrated with indium and zinc according to ASTM D3417 and D3418. All measurements were carried out in nitrogen atmosphere. The non isothermal process was evaluated. The sample was heated to 300°C, held for 5 min at this temperature, then cooled and heated at constant rates of 10°C/min. The crystallization (T_c) and melting temperatures (T_m) were obtained by cooling and heating curves, respectively. The degree of crystallinity was calculated considering the weight fraction of polymer and the heat of fusion of 100% crystalline PP and PET. The relative degree of crystallinity (X_c) was already discuss in another paper.[22] X_c as function of the temperature is defined as:

$$X_c = \frac{\int_{T_o}^{T} (dH_c/dT)dT}{\int_{T_0}^{T_\infty} (dH_c/dT)dT}$$

where, T_0 and T_∞ are the onset and endset crystallization temperatures, respectively, and dH_c/dT is the heat flow.

AFM experiments were performed a Nanoscope IIIa-Digital Instruments. AFM images were obtained under ambient conditions while operating the instrument in the intermitent mode, using ultramicrotomed surfaces. Silicon probes (Nanoprobes, Digital Instruments) were used at their fundamental resonance frequencies which typically varied from 170 to 210 kHz depending on the cantilever. The topographic and phase images were obtained.

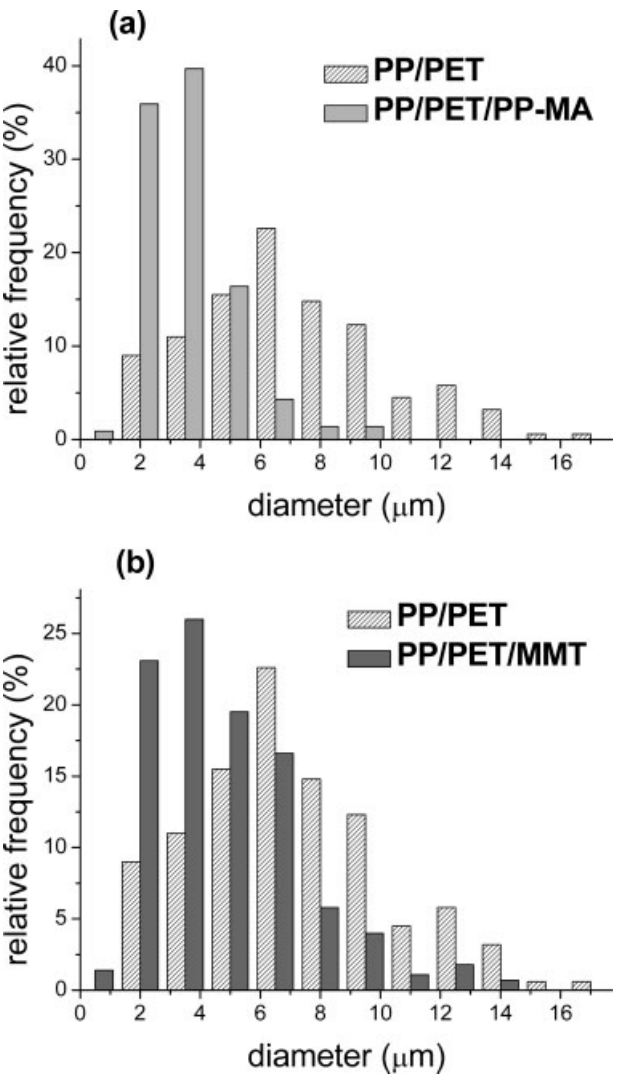

Figure 3 Distribution of the PET domains diameters in the (a) PP/PET and PP/PET/PP-MA blends and (b) PP/PET and PP/PET/clay.

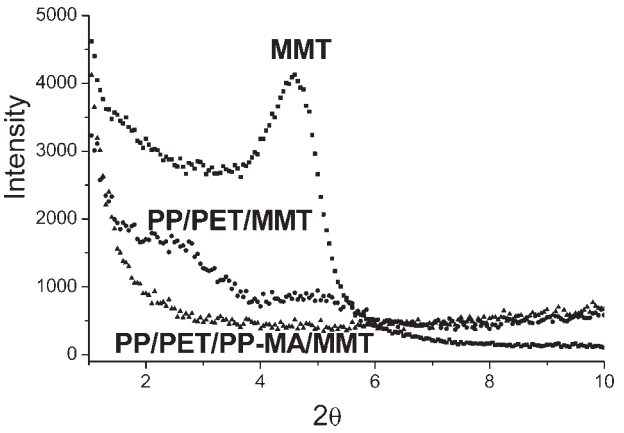

Figure 4 Comparative WAXD between MMT, PP/PET/clay, and PP/PET/PP-MA/clay.

RESULTS AND DISCUSSION

The effect of the compatibilizer in the blends morphology

PP and PET are immiscible polymers and therefore, distinct phases are observed by SEM. A typical morphology of the blends is shown in the Figure 1. The blend shows spherical domains of PET. Cavities [Fig. 1(b)] are also observed in the fractured surface indicating removal of PET balls. PET domains easily debond and detach from the PP matrix due to the poor interfacial adhesion between them. Nevertheless, the compatibilized PP/PET blend show good interfacial adhesion between the phases as visualized by SEM [Fig. 1(c–d)]. The coarse dispersion of PET became markedly finer owing to presence of the compatibilizer [Fig. 1(c)]. It can be observed that the surface of the PET domains present different aspect

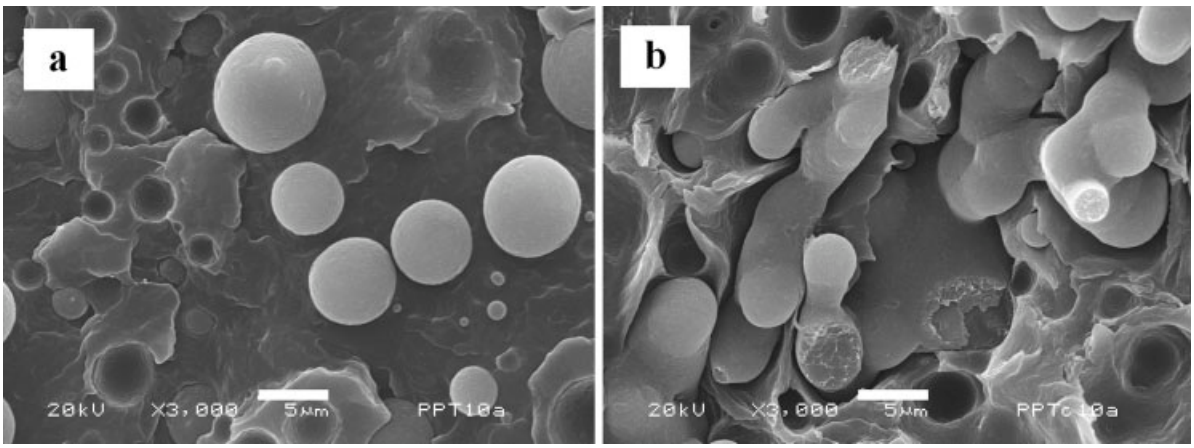

Figure 5 Morphology of the PET domains in the (a) PP/PET/clay; (b) PP/PET/PP-MA/clay (interconnected morphology).

when PP-MA was used. It seems that it recovery the PET domains [Fig. 1(d)]. The interfacial adhesion was also investigated by AFM. The Figure 2 shows the topographic and phase images obtained from PP/PET and PP/PET/PP-MA. The PET domain in the uncompatibilized blend [Fig. 2(a)], as shown before, is detached from the PP matrix. In the compatibilized blend [Fig. 2(b)] it is possible to observe the adhesion of the phases. The compatibilizer, located in the interphase, may act as an adhesion promoter between the PP and PET phases.

The PET domains in the PP/PET blend are bigger than compatibilized blend. In general the dispersion was poor with a wide distribution of diameters of the PET domains in the uncompatibilized blend [Table I and Fig. 3(a)].

The final size of the dispersed phase is determined by the competition between coalescence and breakup. It can be observed the coalescence of the PET domains in some extension [Fig. 1(a)] and both effects must have occurred in this sample. A homogeneous morphology was observed in the

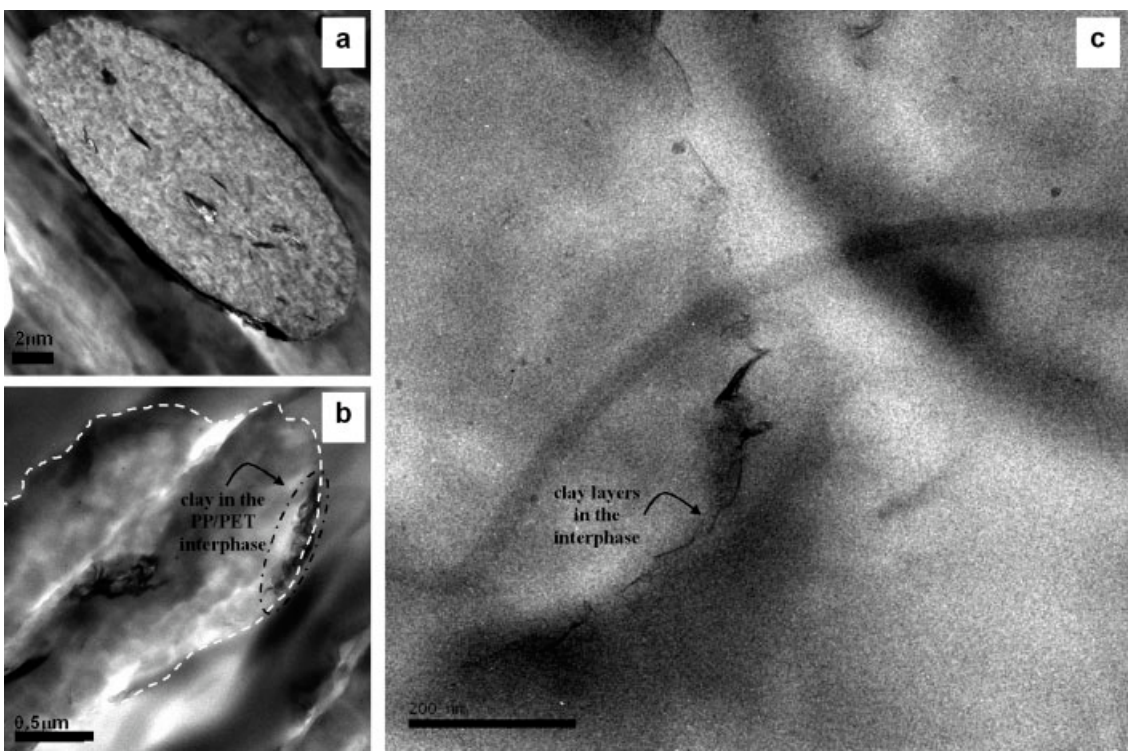

Figure 6 TEM micrographies of the PP/PET/clay (a,b) and PP/PET/PP-MA/clay (c).

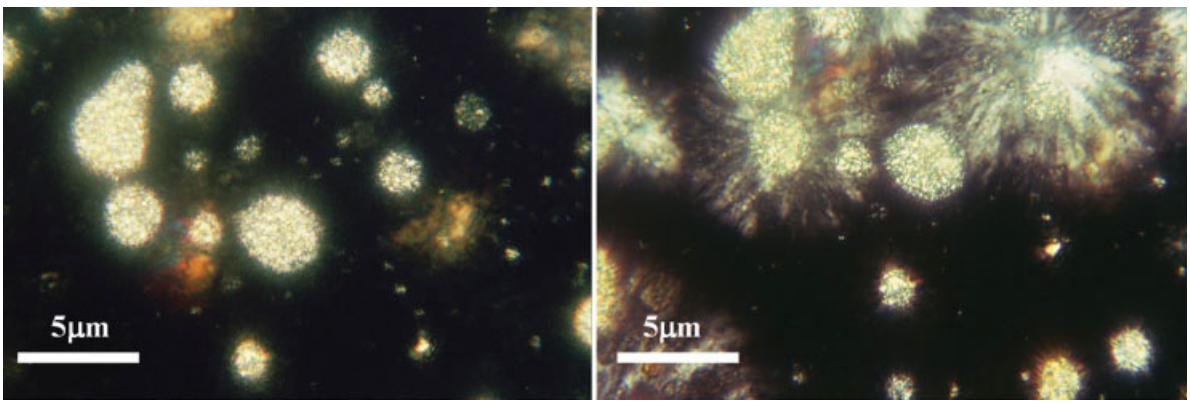

Figure 7 PP crystallization on the PET domains in the PP/PET/PP-MA blend. [Color figure can be viewed in the online issue, which is available at www.interscience.wiley.com.]

compatibilized blend [Fig. 1(c)]. The addition of the compatibilizer reduces the PET domains sizes resulting in a narrow distribution of sizes in the blend [Table I and Fig. 3(a)]. The average particle size decreased from about 6.3 μm in PP/PET to about 2.7 μm in PP/PET modified with PP-MA.

Morphology of the nanocomposites

A decrease in the degree of coherent layer stacking (i.e., a more disordered system) in the clay would lead to peak broadening and intensity loss in WAXD. The absence of the signal in WAXD suggests that clay morphology is exfoliated when PP-MA was used (Fig. 4). For the uncompatibilized system, WAXD peak are shifted to lower angles, indicating the increase in interlayer spacing from 19.2 to 44.1 Å by the intercalation of polymer.

Similar to PP/PET blends, the uncompatibilized nanocomposite shows also spherical domains of PET [Fig. 5(a)]. An average size of about 4.0 μm was observed, whereas a decrease in particles size was obtained for PP/PET modified with clay [Table I and Fig. 3(b)].

The reduction of the particle size can be related to the dispersion of the clay in the interfacial region, that may act as a compatibilizer and hinder the coalescence.[15] Although the clay was located in the interfacial region of the blend, the PET domains seem unattached in the PP matrix (see Fig. 5). In this way, the exclusive use of the MMT does not result in a good compatibilization of the PP and PET phases.

The TEM micrographs show clearly the clay particles (Fig. 6). In the uncompatibilized nanocomposite, the clay particles are big and they are situated in the interphase and in the PET domains [Fig. 6(a,b)]. When PP-MA was used, the clay particles are smaller than in the uncompatibilized nanocomposite. Under higher magnifications it was possible to observe individual layers situated in the interphase [Fig. 6(c)]. The clay was predominantly located in the interphase and in the PET phase in all nanocomposites. Using polar polymers (or polymer containing fuctional groups) favorable interactions with the surface of clay may occur, and that aid the intercalation/exfoliation process.[18,21] Thus, the maleic anhydride groups in the PP-MA should be

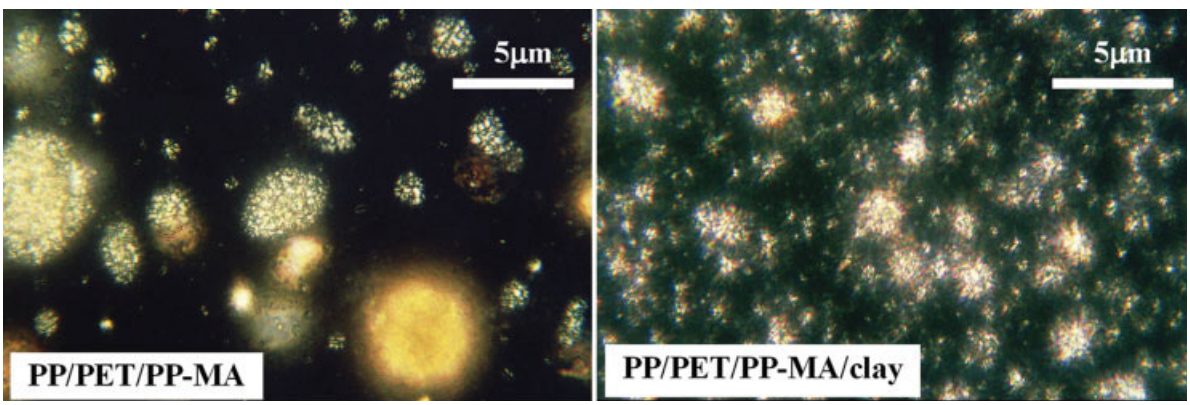

Figure 8 PET crystallization process by POM (a) PP/PET/PP-MA and (b) PP/PET/PP-MA/clay. [Color figure can be viewed in the online issue, which is available at www.interscience.wiley.com.]

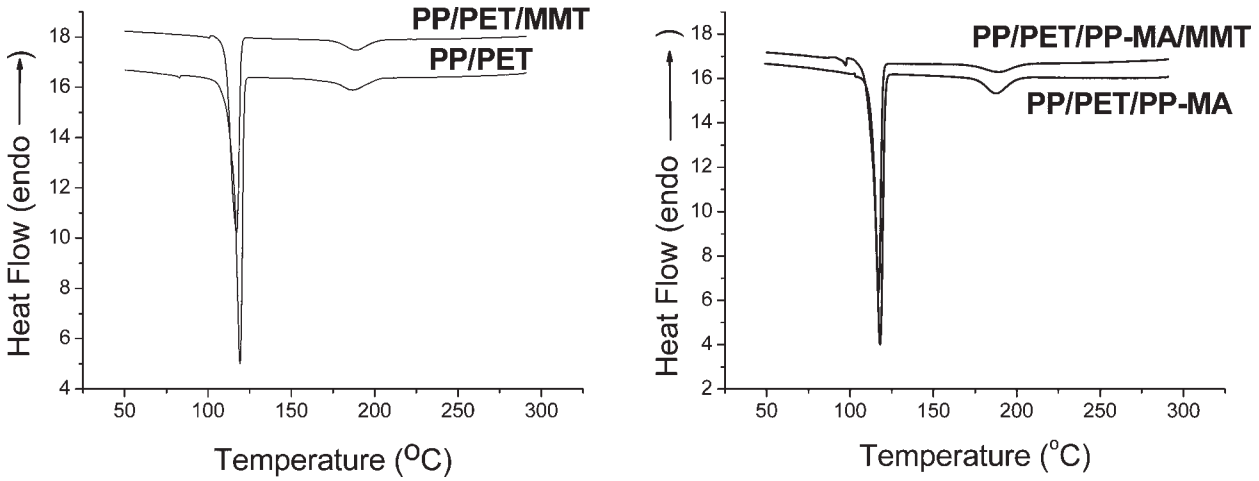

Figure 9 DSC crystallization curves of blends.

facilitating the dispersion of the clay layers. The preferential migration of clay to one of the phases and to the interphase has been observed in PP/PA and PBT/PE blends.[13,23]

The PP/PET/PP-MA/clay presents quite different morphology for PET domains by SEM. They take over a complex three-dimensional arrangement [Fig. 5(b)]. The PET domains are interattached in larger extension. In this sample, it seems that the coalescence has a dominant effect. Apparent decohesion between PP and PET phases was observed for this sample. A similar morphology was also observed in the PP/PS nanocomposite.[15]

Thermal and crystallization behavior

The Table I shows the thermal and crystallization behavior of PP/PET blends. The T_m of the PP and PET remains unmodified in these blends. The T_c for the PP phase in the blends was slightly smaller than the pure PP, and the T_c of the PET phase was slightly higher than the pure PET. In the blends, the T_c value was pratically constant and it is not influenced by clay and/or compatibilizer addition. The crystallinity degree in PP and PET phases remained similar in the blends. The crystallinity degree of PP was higher in the blends when compared to pure PP that can be explained by the higher nucleation density induced by the PET domains. PET domains were the start point to PP crystallization in the blends (Fig. 7). A great number of PET nuclei were observed in the PP/PET nanocomposites (Fig. 8).

The Figure 9 shows the DSC crystallization curves of blends. The development of the relative degree of crystallinity (X_c) with the time (t) can be determinated for nonisothermal process.[22] The crystallization time was separately evaluated for PP and PET phases. Several studies have been demonstrated that the clay has a nucleant effect in the nanocomposites, increasing its crystallization rate.[11] However, the presence of clay in both blends (with and without compatibilizer) resulted in a decrease of crystallization

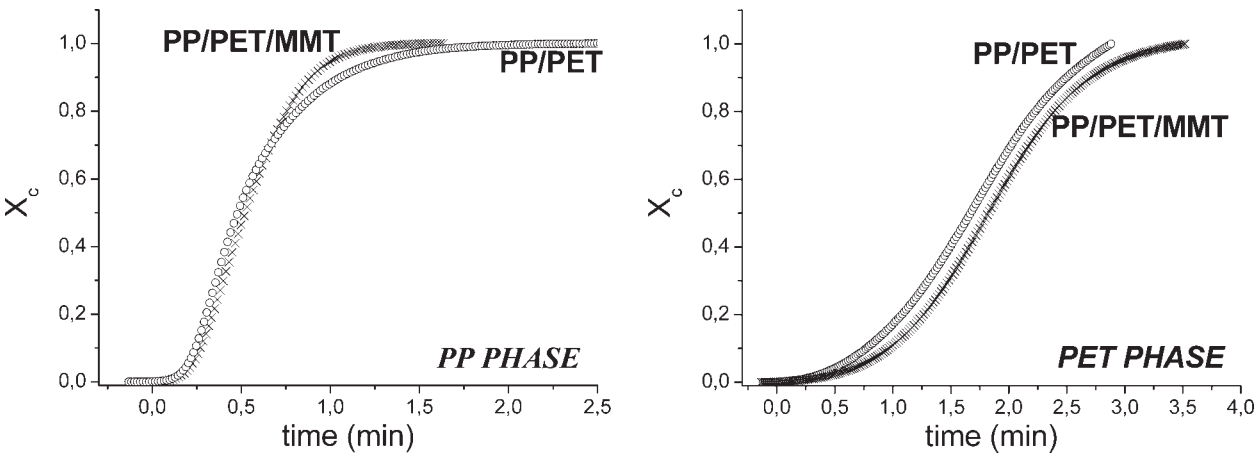

Figure 10 Development of relative crystallinity (X_c) of the uncompatibilized blends.

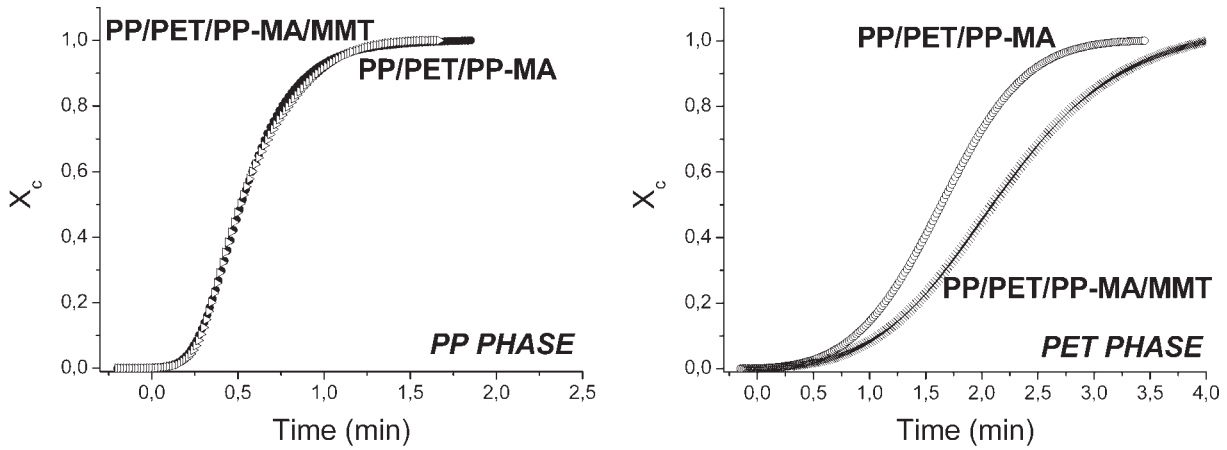

Figure 11 Development of relative crystallinity (X_c) of the compatibilized blends.

rate of the PET phase (Figs. 10 and 11). This effect is more evident in the compatibilized blend (Fig. 11).

As observed early, the incorporation of compatibilizer facilitated the dispersion of the clay in the PP/PET, where the clay mainly is located in the PET phase than PP phase. In the nanocomposite with exfoliated morphology, the retardation of the crystallization rate can be related to the higher clay content in PET phase that difficult the crystallization process.

CONCLUSIONS

In the PP/PET blends and nanocomposites, the PET domains usually presented spherical shapes, and they were the start point to PP crystallization. The addition of compatibilizer and/or clay reduced the diameter of dispersed phase. The nanocomposite containing PP-MA lead to an interconnected morphology and the PET domains were detached from the PP matrix. The incorporation of compatibilizer facilitated the dispersion of the clay in the PP/PET and the clay particles are smaller than in the uncompatibilized nanocomposite. In the all nanocomposites, the clay was predominantly located in the interphase and in the PET phase. The retardation of the crystallization rate of the PET was observed. This behavior can be related to the higher clay content in PET phase that difficult the crystallization process.

References

1. Alexandre, M.; Dubois, P. Mater Sci Eng 2000, 28, 1.
2. Ray, S. S.; Okamoto, M. Prog Polym Sci 2003, 28, 1539.
3. Manias, E.; Touny, A.; Wu, L.; Strawhecker, K.; Lu, B.; Chung, T. C. Chem Mater 2001, 13, 3516.
4. Ahmadi, S. J.; Huang, Y. D.; Li, W. J Mater Sci 1919 2004, 39.
5. Százdi, L.; Pukánszky, B., Jr.; Vancso, G. J.; Pukánszky, B. Polymer 2006, 47, 4638.
6. Quintanilla, M. L. L.; Valdés, S. S.; Valle, L. F. R.; Miranda, R. G. Polym Bull 2006, 57, 385.
7. Dennis, H. R.; Hunter, D. L.; Chang, D.; Kim, S.; White, J. L.; Cho, J. W., et al. Polymer 2001, 42, 9513.
8. Chen-Yang, Y. W.; Yang, H. C.; Li, G. J.; Li, Y. K. J Polym Res 2004, 11, 275.
9. Peeterbroeck, S.; Alexandre, M.; Jérôme, R.; Dubois, P. Polym Degrad Stab 2005, 90, 288.
10. Pegoretti, A.; Kolarik, J.; Peroni, C.; Migliaresi, C. Polymer 2004, 45, 2751.
11. Calcagno, C. I. W.; Mariani, C. M.; Teixeira, S. R.; Mauler, R. S. Polymer 2007, 48, 966.
12. Gahleitner, M.; Kretzschmar, B.; Van Vliet, G.; Devaux, J.; Pospiech, D.; Bernreitner, K.; Ingolic, E. Rheol Acta 2006, 45, 322.
13. Chow, W. S.; Bakar, A. A.; Ishak, Z. A. M.; Kocsis, J. K.; Ishiaku, U. S. Eur Polym J 2005, 41, 687.
14. Zaragoza, M. V.; Vargas, E. R.; Rodríguez, F. J. M.; Martínez, B. M. H. Polym Degrad Stab 2006, 91, 1319.
15. Ray, S. S.; Pouliot, S.; Bousmina, M.; Utracki, L. A. Polymer 2004, 45, 8403.
16. Neogi, S.; Hashmi, S. A. R.; Chand, N. Bull Mater Sci 2003, 26, 579.
17. Ding, C.; Jia, D.; He, H.; Guo, B.; Hong, H. Polym Test 2005, 24, 94.
18. Lertwimolnun, W.; Vergnes, B. Polymer 2005, 46, 3462.
19. Modesti, M.; Lorenzetti, A.; Bon, D.; Besco, S. Polym Degrad Stab 2006, 91, 672.
20. Bertin, F.; Canetti, M.; Audisio, G.; Costa, G.; Falqui, L. Polym Degrad Stab 2006, 91, 600.
21. Százdi, L. Pukánszky, B. Jr.; Földes, E.; Pukánszky, B. Polymer 2005, 46, 8001.
22. Xu, W. B.; Zhai, H. B.; Guo, H. Y.; Zhou, Z. F.; Whitely, N.; Pan, W. P. J Therm Anal Calorim 2004, 78, 101.
23. Hong, J. S.; Kim, Y. K.; Ahn, K. H.; Lee, S. J.; Kim, C. Rheol Acta 2007, 46, 469.